Phase Separation in Short-Chain Lecithin/Gel-State Long-Chain Lecithin Aggregates†

Jinru Bian and Mary F. Roberts*
Department of Chemistry, Boston College, Chestnut Hill, Massachusetts 02167
Received March 14, 1990; Revised Manuscript Received May 10, 1990

ABSTRACT: Small bilayer particles form spontaneously from gel-state long-chain phospholipids such as dipalmitoylphosphatidylcholine and 0.2 mol fraction short-chain lecithins (e.g., diheptanoylphosphatidylcholine). When the particles are incubated at temperatures greater than the T_m of the long-chain phosphatidylcholine (PC), the particles rapidly fuse (from 90-Å to ≥5000-Å radius); this transition is reversible. A possible explanation for this behavior involves patching or phase separation of the short-chain component within the gel-state particle and randomization of both lipid species above T_m. Differential scanning calorimetry, ^{1}H T_1 values of proteodiheptanoyl-PC in diheptanoyl-PC-d_{26}/dipalmitoyl-PC-d_{62} matrices of varying deuterium content, solid-state ^{2}H NMR spectroscopy as a function of temperature, and fluorescence pyrene excimer-to-monomer ratios as a function of mole fraction diheptanoyl-PC provide evidence that such phase separation must occur. These results are used to construct a phase diagram for the diheptanoyl-PC/dipalmitoyl-PC system, to propose detailed geometric models for the different lipid particles involved, and to understand phospholipase kinetics toward the different aggregates.

Small bilayer particles of gel-state phosphatidylcholines (PC's)[1] are, in general, unstable. It has been documented that small unilamellar vesicles of dipalmitoyl-PC are unstable below T_m and fuse to form large unilamellar vesicles (Lichtenberg et al., 1981; Schullery et al., 1980). The curvature necessary for forming small unilamellar vesicles is too much of a strain for the gel-state PC system. Bilayer disks of gel-state PC's, such as those formed with bile salts or apoproteins, are also unstable; with these systems, particle size depends dramatically on the ratio of PC to additive. Short-chain PC's, with 12–18 carbons in both chains, induce formation of small particles from multilamellar gel-state dipalmitoyl-PC. The particles produced at 20 mol % short-chain PC have been shown to be thermodynamically stable below T_m with properties consistent with gel-state PC bilayers (Gabriel & Roberts, 1984, 1986, 1987). The encapsulation volumes of the gel-state particles are smaller than expected for 200-Å diameter spherical vesicles (Roberts & Gabriel, 1987), suggesting that geometries other than spherical vesicles (e.g., bilayer disk) may be present. The particles with 20–33 mol % diheptanoyl-PC are nonlytic to human erythrocytes from 10 to 45 °C, while monomers or micelles of the short-chain PC's (and other detergent micelles) are extremely lytic, indicating that classical mixed micelles do not exist in this composition range. Above the phase transition temperature of the long-chain PC, particles rapidly fuse to large multilamellar structures (Eum et al., 1989); this structural change is reversible upon decreasing the temperature. A possible explanation for this behavior is that in the small particles the two lipids are phase-separated, but mix randomly when the long-chain PC becomes liquid-crystalline. This binary PC system, while complex, has the potential for reconstitution of membrane-bound proteins and is also a unique substrate system for water-soluble phospholipases (Gabriel et al., 1987). In this work, we present DSC, NMR, and fluorescence evidence for phase separation of the short-chain PC from long-chain PC in particles with gel-state dipalmitoyl-PC. The phase behavior of the diheptanoyl-PC/dipalmitoyl-PC system is examined quantitatively as a function of mole fraction short-chain PC and temperature. The results explain the temperature-induced fusion of binary PC particles, the preferential activity of water-soluble phospholipases toward the short-chain PC in these particles, and the unusual temperature dependence of the enzymatic reactions.

Experimental Procedures

Chemicals. Dipalmitoyl-PC, dipalmitoyl-PC-d_{62}, and diheptanoyl-PC were obtained from Avanti Polar Lipids, Inc., in chloroform and used without further purification. Diheptanoyl-PC-d_{26} was synthesized with carbonyldiimidazole as described previously (DeBose et al., 1985). Pyrene (>99%) was obtained from Aldrich.

Preparation of Aqueous Lipids. Appropriate aliquots of PC stock solutions in chloroform were transferred to glass vials and dried under nitrogen. For fluorescence studies, a stock pyrene in chloroform solution was prepared, and aliquots were added to the lipid samples in chloroform. The resultant lipid films were lyophilized overnight to remove any remaining trace of organic solvent prior to hydration with distilled deionized water. Upon hydration, the sample was incubated above 40 °C for 5 min and then cooled down to room temperature. This process produces a very homogeneous mix of small particles as detected by quasi-elastic light scattering (Eum et al., 1989).

Fluorescence Spectroscopy. Fluorescence emission was monitored at room temperature (unless otherwise indicated) with a Shimadzu RF5000V spectrofluorometer using the high-sensitivity setting and 3-nm bandwidth. The excitation wavelength was 360 nm. Light scattering was not a problem with these samples since there was no effect on the fluorescence intensity ratio when the light path was altered. Samples were not deoxygenated. Two types of experiments were run: (i) fixed mole fraction of pyrene and 25 mM total dipalmitoyl-PC plus diheptanoyl-PC; (ii) fixed ratio of pyrene to diheptanoyl-PC with variation in the total PC content. Since it takes time for the binary PC systems to reach equilibrium after heating and cooling, we did not deoxygenate samples. This

† This work is supported by NIH Grant GM 26762.
* To whom correspondence should be addressed.

[1] Abbreviations: diacyl-PC, 1,2-diacyl-*sn*-glycero-3-phosphocholine; DSC, differential scanning calorimetry.

0006-2960/90/0429-7928$02.50/0

will not affect the interpretation of results since the saturation of oxygen in all samples will be the same, and the lifetime and intensity of pyrene fluorescence are linear functions of oxygen content relative to their values in oxygen-free systems (Chong & Thompson, 1985).

NMR Spectroscopy. ^{1}H longitudinal relaxation times (T_1) were measured at 300 MHz by inversion recovery (Vold et al., 1968) using a Varian XL-300 spectrometer. Sample temperature was 30 °C. Spectral parameters included a 90° pulse width of 20 μs, 1800-Hz sweep width, 8000 data points, 4.0-s recycle delay, 40–320 transients per spectrum depending on the proton content of the sample, and 8–9 t values for each T_1 experiment. ^{2}H NMR (76.8 MHz) spectra were obtained at the Chemistry Department of the California Institute of Technology, on a Bruker WM 500 spectrometer described by Watnick et al. (1990). The 100 mM dipalmitoyl-PC/5 mM diheptanoyl-PC-d_{26} sample (100 μL) was prepared in ^{2}H-depleted H_2O and sealed in a tube. Spectra were acquired by using a quad echo sequence; parameters included a 90° pulse width (3.5 μs), 167-kHz sweep width, 1K data points, and 1000–7000 transients accumulated.

Differential Scanning Calorimetry. Calorimetric studies were performed with a Perkin-Elmer DSC-2D/TADS SYSTEM differential scanning calorimeter using a heating (or cooling) rate of 1 °C/min. In all runs, the amount of dipalmitoyl-PC and the sample volume were kept constant, while the amount of diheptanoyl-PC added was varied.

Results

Effect of Diheptanoyl-PC on the ΔH and T_m of Dipalmitoyl-PC. Preliminary DSC studies of diheptanoyl-PC/long-chain PC mixtures showed little effect of 20 mol % short-chain component of the T_m of dipalmitoyl- and distearoyl-PC (Gabriel & Roberts, 1986). The effect on ΔH had not been quantified. We have measured the ΔH (as well as T_m) for melting a fixed amount of dipalmitoyl-PC with 0–0.7 mol fraction diheptanoyl-PC added. As can be seen in Figure 1A, addition of <10 mol % diheptanoyl-PC had only a small effect on the phase transition enthalpy. Between 10 and 20 mol % short-chain PC, the ΔH decreased to about one-third the original value. In this same region, there was no significant effect on the T_m (Figure 1B). From 20 to 40 mol % diheptanoyl-PC, both ΔH and T_m were almost constant, suggesting that in this region distinct dipalmitoyl-PC particles are formed. Because a ΔH was observed with this much diheptanoyl-PC, some or all of it must be phase-separated from the dipalmitoyl-PC matrix. Between 40 and 50% short-chain PC, both ΔH and T_m decreased. Above 60 mol % diheptanoyl-PC, no ΔH was detected. Previous work has indicated that mixed micelles which are lytic to erythrocytes are the dominant structures in this regime (Gabriel et al., 1987). In these mixed micelles, the dipalmitoyl-PC must not pack into units which cooperatively give rise to a detectable phase transition since ΔH is decreased below the detection of the instrument. This abrupt decrease in ΔH around 60 mol % diheptanoyl-PC suggests the onset of a classical mixed micelle phase with little interaction of the long-chain species and with no coexisting bilayer species.

^{1}H Spin–Lattice Relaxation Times of Diheptanoyl-PC in Binary PC Mixtures. The strength of the proton dipole is about 7 times of that of a deuteron. If the ^{1}H relaxation of short-chain PC protons is dominated by inter- as well as intramolecular dipolar mechanisms, the T_1's of these protons should be smaller (e.g., more effective relaxation rate, $1/T_1$) in a proton-rich environment than in a deuteron-rich environment. The T_1 values for several well-resolved diheptanoyl-PC protons in a dipalmitoyl-PC-d_{62} (20 mM) matrix with varying amounts of heptanoyl-PC-d_{26} are shown in the left-hand side of Figure 2 (open symbols). The only chains with protons belong to the short-chain PC in this region. The total concentration of diheptanoyl-PC was 5 mM; the mole fraction of proteo chains was varied from 0.02 to 0.1 of the total phospholipid. For all protons but the terminal methyl group, T_1 decreased as the proton content increased. The T_1 changes were smaller and in the opposite direction for a comparable experiment looking at short-chain PC T_1 values for a fixed amount of diheptanoyl-PC (0.025 mol fraction) with varying proteodipalmitoyl-PC content (0.225–0.425 mol fraction total phospholipid). In this experiment, the diheptanoyl-PC T_1 values were smaller in magnitude than for that amount of short-chain PC in a perdeuterated dipalmitoyl-PC matrix, suggesting that there is some influence of the long-chain PC on the diheptanoyl-PC. As the relative amount of proteodipalmitoyl-PC increased, the T_1s increased rather than decreased. This could indicate a change in the particle size (to a smaller structure) or geometry between having the major component long-chain PC in an all-deuterated or mostly protonated form. QLS measurements detected only minor changes in the size of the particles with perdeuterated chains. Another possible explanation for the increase in T_1 of the short-chain PC when proteo long chain was added is that the proteo long-chain PC contributes intensity, although broad, that interferes and biases the short-chain T_1 measurements. In any case, if both PC species were not extensively phase-separated, the decrease in T_1 with increasing proton content of the minor component (0.2 mol fraction diheptanoyl-PC) would have been considerably smaller, or a greater effect should have been observed with the variation in dipalmitoyl-PC-d_{62}.

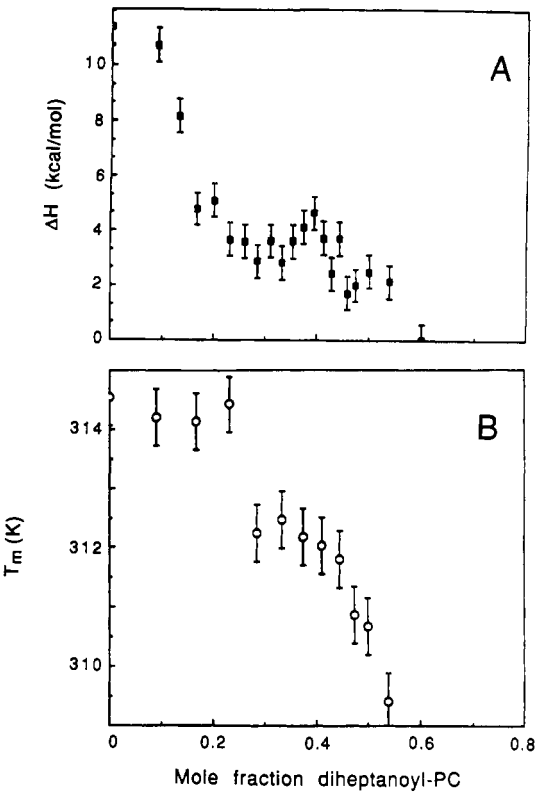

FIGURE 1: Enthalpy (A) and transition temperature (B) as determined by DSC for the gel-to-liquid-crystalline phase transition of a fixed concentration of dipalmitoyl-PC (100 mM) with increasing mole fraction diheptanoyl-PC.

^{2}H NMR of Binary Lipid Mixtures. ^{2}H NMR spectroscopy is an excellent technique for obtaining the time-averaged

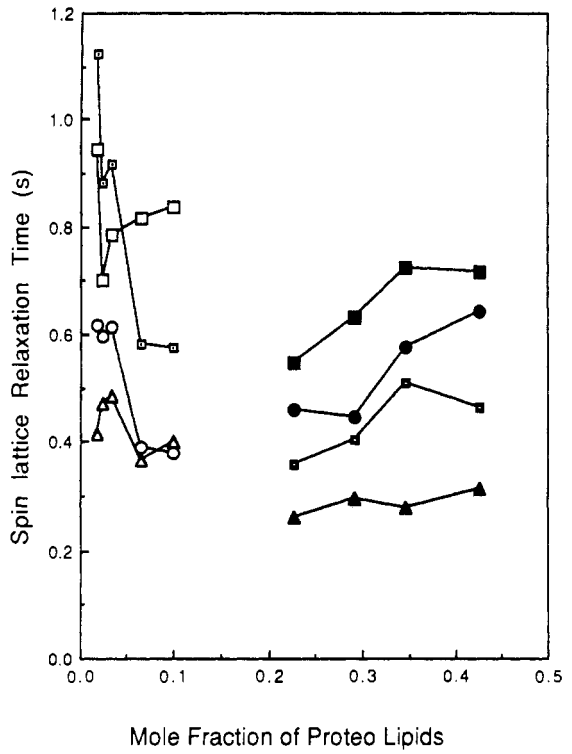

FIGURE 2: ^{1}H spin–lattice relaxation times (T_1) for bulk methylene (⊡), terminal methyl (□), α-CH_2 (○), and $N(CH_3)_3$ (△) protons of diheptanoyl-PC in a dipalmitoyl-PC matrix as a function of the mole fraction of protonated lipids. The open symbols are for varying ratios of diheptanoyl-PC/diheptanoyl–PC-d_{26} (total concentration 5 mM) in a chain-perdeuterated 20 mM dipalmitoyl-PC matrix. The closed symbols are for a fixed concentration of proteodiheptanoyl-PC (0.625 mM) with 4.375 mM diheptanoyl-PC-d_{26} and different ratios of dipalmitoyl-PC to dipalmitoyl-PC-d_{62} (total concentration at 20 mM with the proteo compound from 5 to 10 mM).

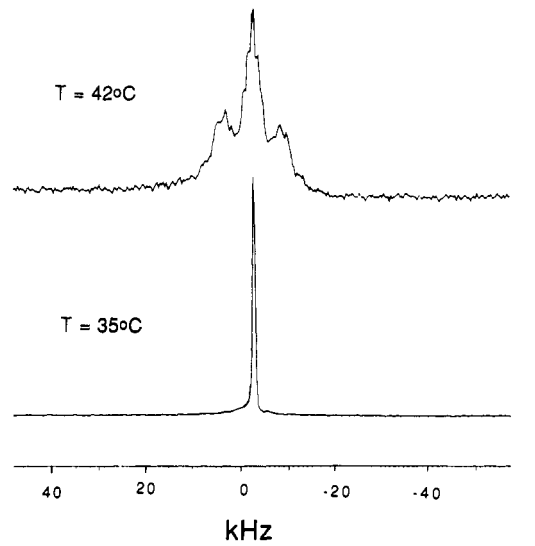

FIGURE 3: ^{2}H NMR spectra (76.8 MHz) of diheptanoyl-PC-d_{26} mixed with a 20-fold excess of dipalmitoyl-PC at (bottom) 35 °C and (top) 42 °C.

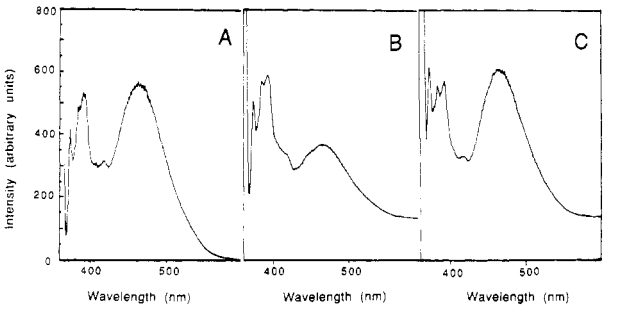

FIGURE 4: Fluorescence spectra of 3 mol % pyrene in (A) 25 mM diheptanoyl-PC, (B) 13.6 mM diheptanoyl-PC/11.4 mM dipalmitoyl-PC particles, and (C) 25 mM dipalmitoyl-PC large unilamellar vesicles. Excitation was at 360 nm.

orientation of methylene segments of short-chain PC molecules in the vicinity of dipalmitoyl-PC (or another long-chain lipid) as long as the particle is multilamellar (Seelig, 1980; Brown, 1982). This allows us to assess the phase behavior of short-chain PC in the presence of excess long-chain PC. When 5 mol % diheptanoyl-PC-d_{26} is mixed with dipalmitoyl-PC at temperatures below the T_m of the long-chain component, only an isotropic line is observed; this is observed even when the water content of the sample is decreased (to about 80%) from the original 100 mM dipalmitoyl-PC/5 mM diheptanoyl-PC sample (Figure 3, bottom scan). Under these conditions, most of the short-chain PC can be separated from the multilamellar dipalmitoyl-PC by centrifugation. The particles in the supernatant are ~90-Å R_H and have a 4–5/1 stoichiometry of long-chain PC to short-chain PC (Riedy et al., unpublished results). Even with a large excess of dipalmitoyl-PC multibilayers, almost all of the short-chain PC is present as small particles with a nearly fixed composition of gel-state dipalmitoyl-PC. Hence, multibilayers coexist with small binary PC bilayer aggregates. When the sample temperature is increased to 40 °C or above, a powder pattern is detected for the deuterated short-chain PC (Figure 3, top scan). A sharp feature is still visible in the ^{2}H NMR spectrum. While there may be a contribution to this from some isotropic component (short-chain PC in small particles), the line width is not quite as narrow as for perdeuterated diheptanoyl-PC at 35 °C. The sharp feature may more reasonably represent diheptanoyl-PC-d_{26} molecules with motional averaging over a resticted angular range in multibilayers. Since these mixtures are not lytic to red blood cells (Gabriel et al., 1987), any small structures cannot be classical micelles. The largest residual quadrupolar splitting is ±8 kHz. Presumably this splitting belongs to the initial CD_2 segment of the *sn*-2 chain. For comparison, the residual splitting of liquid-crystalline dipalmitoyl-PC specifically labeled at C-4 of the fatty acyl chain is ±12.8 kHz (Brown & Davis, 1981). Thus, even when they are intimately mixed in a liquid-crystalline bilayer with the long-chain species, the short-chain PC chains are much less ordered.

Pyrene Fluorescence in Diheptanoyl-PC/Dipalmitoyl-PC Aggregates. Pyrene fluorescence spectra can provide evidence for differences in environments in lipid aggregates. Typical fluorescence spectra of pyrene in diheptanoyl-PC, dipalmitoyl-PC, and diheptanoyl-PC/dipalmitoyl-PC systems are shown in Figure 4. The peak at 392 nm monitors pyrene monomer fluorescence, and the peak at 466 nm is from pyrene excimer. The intensity ratio of excimer to monomer (I_{466}/I_{392}) depends on the microenvironment of pyrene, and hence this ratio is an indicator of the microstructure of the system. Excimer formation in fluid media is a diffusion-controlled process (Galla & Sackman, 1974), and every collision between excited monomer and ground monomer in ordinary organic solvent leads to excimer formation (Birks et al., 1963). The dissociation constant of the pyrene excimer is small compared to the transition rate $1/\tau$ of the complex into two unexcited molecules (Forster, 1969). This implies that the ratio of excimer intensity (466 nm) to monomer intensity (392 nm) can be expressed as $I_{466}/I_{392} = \alpha\kappa k_a \tau c$, where α is a constant depending on molecular size, κ is a correction coefficient for using the intensity rather than quantum yield ratio, τ is ex-

cimer lifetime, k_a is the second-order rate constant, and c is the concentration of unexcited probe. Thus, for a system to have pyrene excimer fluorescence diffusion-controlled, I_{466}/I_{392} should be proportional to the pyrene concentration (Galla, & Sackman, 1974).

The behavior of diheptanoyl-PC micelles as a function of PC concentration has been studied in detail by light scattering (Tausk et al., 1974; Burns et al., 1983) and SANS (Lin et al., 1987). Near the cmc (1.5 mM), the micelles are small structures; as [PC] increases, the micelles grow from spherical structures to rods with a moderate degree of polydispersity. Pyrene fluorescence in this system serves as a control for the diheptanoyl-PC/dipalmitoyl-PC binary mixtures. The excited monomer of pyrene has a lifetime of about 500 ns (Moigne et al., 1988) in organic media. If the micelles are small and the pyrene concentration is low, the average number of pyrene molecules in one particle is low, so there is a low probability that an excited monomer will interact with another pyrene molecule to form an excimer even though monomer has a sufficiently long lifetime to sample the entire particle. The solubility of pyrene in water is extremely low, so the only way for monomers to interact is through micelle collisions. If the micelles grow, the average number of pyrene molecules in one micelle increases, and the probability of excimer formation is increased. This is indeed what is observed in Figure 5A. The ratio of pyrene to diheptanoyl-PC has been kept constant in this experiment, and the total lipid concentration increased. I_{466}/I_{392} for 3% pyrene was about twice that for 1.5% pyrene, indicating diffusion control. Below 5 mM diheptanoyl-PC, this ratio increased slowly, suggesting that particle size was not increasing significantly. Between 5 and 20 mM lipid, the slope of I_{466}/I_{392} as a function of PC concentration increased (1.5-fold). If there were not a microstructure change in the micellar system in this concentration range, the ratio of the two intensities should be constant. In fact, small-angle neutron scattering studies have shown that the diheptanoyl-PC micelle average size grows significantly from 5 to 20 mM (Lin et al., 1987). The slope of the excimer/monomer curve decreases above 20 mM for 1.5% pyrene, indicating that further micelle size changes are not significantly altering the number of pyrene molecules per micelle, and hence the probability of excimer formation. The pyrene fluorescence behavior as a function of diheptanoyl-PC concentration is similar to what has been observed for SDS micelles (Kim et al., 1981). Those detergent micelles also grow as polydisperse rods with increasing detergent concentration.

The pyrene intensity ratio can also be used to probe the microstructure change when dipalmitoyl-PC is added to the system. Changes in the slope of I_{466}/I_{392} as a function of mole percent diheptanoyl-PC indicate structural changes in particles. Because the long-chain PC is in a gel state, the pyrene may be preferentially solubilized in a specific domain, presumably the short-chain PC. In the first variation of this experiment, the total lipid content was 25 mM with the ratio of pyrene to diheptanoyl-PC kept at 3 mol %. The result is shown in Figure 5B. Clearly, the intensity ratio increased with diheptanoyl-PC content. In contrast to the pure micelle system, the curve is concave. This means the gel-state long-chain PC in the system has influenced the disposition of the diheptanoyl-PC. It also suggests that there are several different particles as the large multilamellar vesicles of pure dipalmitoyl-PC are converted to mixed micelles with diheptanoyl-PC.

A second type of fluorescence experiment involved keeping the total amount of pyrene and the total amount of PC fixed, but varying the mole percent diheptanoyl-PC. Figure 6A

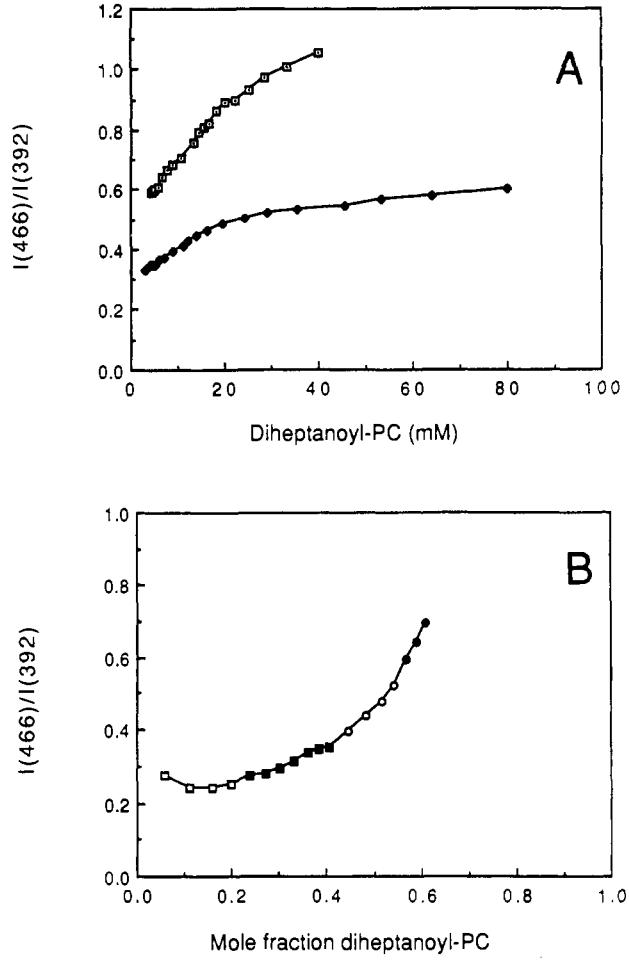

FIGURE 5: Ratio of pyrene excimer (466 nm) to monomer (392 nm) fluorescence intensities in (A) diheptanoyl-PC micelles as a function of lecithin concentration and (B) diheptanoyl-PC/dipalmitoyl-PC particles as a function of mole fraction diheptanoyl-PC. In (A), the ratio of pyrene to diheptanoyl-PC was kept constant: (♦) 1.5 mol % and (□) 3 mol % diheptanoyl-PC. In (B), the ratio of pyrene to diheptanoyl-PC was kept constant at 0.03 while the total amount of PC was kept constant at 25 mM and the ratio of short-chain to long-chain varied. The different symbols break the curve into four regions of different slopes.

shows the rate of I_{466}/I_{392} for different fixed pyrene concentrations as a function of mole percent of diheptanoyl-PC in dipalmitoyl-PC. The shapes of the curves are the same for 0.6–3.0 mol % pyrene, again consistent with diffusion-controlled behavior. Furthermore, I_{466}/I_{392} values are a linear function of pyrene concentration. The complex nature of the curves implies several discrete environments exist in the diheptanoyl-PC/dipalmitoyl-PC system. There are two explanations for the intensity ratio increase in the region where the short-chain PC is less than 20% of the total lipid. (i) As soon as diheptanoyl-PC is added, there is a phase separation of this component from the gel-state long-chain PC and migration of the pyrene from the dipalmitoyl-PC phase into the more mobile diheptanoyl-PC phase. The extent of pyrene migration is determined by the partition coefficient. In the diheptanoyl-PC phase, the pyrene is more concentrated, and hence excimer formation is enhanced. (ii) Another possibility is that the diheptanoyl-PC is not phase-separated from dipalmitoyl-PC but inserted into this matrix in a random fashion. Mixing the two lipids fluidizes the dipalmitoyl-PC, and the excited monomer diffuses more rapidly in the matrix and thus has a higher probability of interacting with another pyrene molecule to form excimer. The first of these two possibilities is more likely for the following reasons. Pyrene has very low

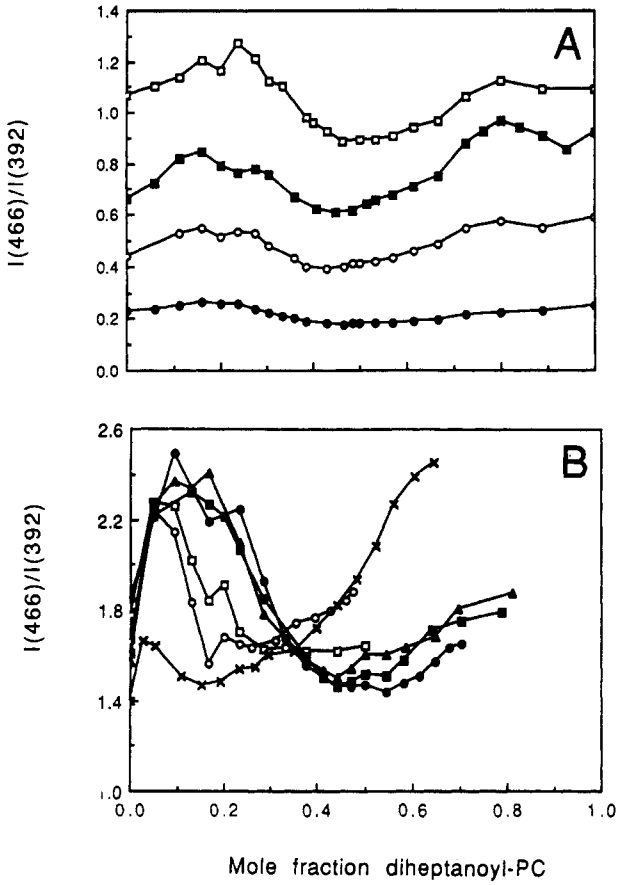

FIGURE 6: (A) Ratio of pyrene excimer (466 nm) to monomer (392 nm) fluorescence intensities as a function of mole fraction diheptanoyl-PC. The pyrene to total lecithin ratio was kept constant at (●), 0.6, (○), 1.4, (■) 2.2, and (□) 3 mol % total lipid (diheptanoyl-PC + dipalmitoyl-PC). (B) The excimer to monomer fluorescence ratio as a function of mole fraction short-chain PC for different temperatures: (■) 23, (▲) 30, (□) 33, (○) 36, and (×) 38 °C. Total PC was 25 mM and pyrene fixed at 1.25 mM.

solubility in gel-state dipalmitoyl-PC (about 0.001) (Galla & Sackman, 1974) with any excess pyrene above the limit "solubilized" in the gel-state PC aggregating into clusters of closely packed molecules (Galla & Sackman, 1974). Microcrystals of pyrene exhibit a high excimer yield because of a sandwichlike arrangement of the molecules in the crystallites which favors the face to face structure necessary for excimer formation (Birks, 1970). If the diheptanoyl-PC sufficiently fluidizes the dipalmitoyl-PC matrix, it should decrease the microclusters and decrease excimer formation. It is difficult to explain the decrease of the intensity ratio after the short-chain PC reaches about 20 mol % if we assume the increase before that point is due to fluidization of the dipalmitoyl-PC matrix. It is much easier to explain the subsequent decrease in the fluorescence data if we assume the phase separation occurs before that point. What follows is that at 20 mol % diheptanoyl-PC a large amount of the pyrene is dissolved in the short-chain PC phase. Any further diheptanoyl-PC added has the effect of diluting pyrene concentration which will decrease the excimer to monomer ratio. This is consistent with the experimental data for the region 20–42 mol % diheptanoyl-PC. There may be two kinds of processes by which diheptanoyl-PC dilutes the total pyrene. As more short-chain PC is added, new diheptanoyl-PC domains form, or more short-chain PC may increase the size of the original diheptanoyl-PC domains. Both processes can dilute pyrene concentration and decrease the excimer to monomer ratio, but the latter process should decrease the ratio more slowly.

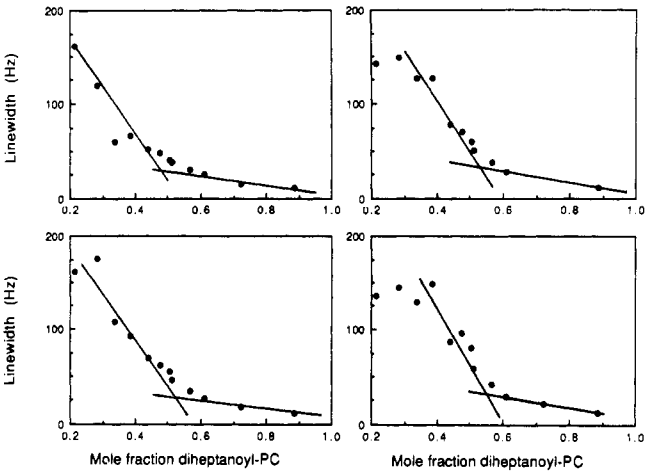

FIGURE 7: ^{1}H line width (Hz) determined at 300 MHz for dipalmitoyl-PC bulk methylene protons in mixtures with diheptanoyl-PC-d_{26} as a function of the mole fraction diheptanoyl-PC: (top left panel) 37, (bottom left) 33, (top right) 30, and (bottom right) 27 °C. The intersection of the two lines is used to determine the mixed micelle single phase boundary.

After a small region in Figure 6A where I_{466}/I_{392} does not change, the excimer to monomer ratio begins to increase again. This can be explained by the existence of a new structural unit, classical mixed micelles formed from diheptanoyl-PC and dipalmitoyl-PC, whose composition is changing. The gel-state long-chain PC should increase the viscosity of the diheptanoyl-PC micelles so diffusion of pyrene monomers in the mixed micelles decreases with increasing dipalmitoyl-PC. Increasing the fraction of diheptanoyl-PC decreases the viscosity of the micelle interior and enhances excimer formation. The region where the intensity ratio does not change may reflect pyrene transfer into mixed micelles smaller in size than the diheptanoyl-PC domains in the bilayer particles. This is a region where classical mixed micelles coexist with bilayer particles.

If one examines the temperature dependence of I_{466}/I_{392} as a function of mole fraction diheptanoyl-PC, one observes parallel behavior (e.g., the same mole fractions of diheptanoyl-PC at fluorescence ratio maxima and minima) for 18–30 °C. Above 30 °C and below 38 °C, both the initial maximum and the minimum in the curve are shifted to lower mole fraction diheptanoyl-PC. The maximum is shifted from 0.2 to 0.1 mol fraction, while the minimum is shifted from 0.5 to 0.3 mol fraction short-chain PC. This correlates with structural changes induced by the dipalmitoyl-PC pretransition. Right around the T_m (38 °C), a completely different profile is obtained.

Mixed Micelle Boundary in Binary PC Mixtures. From the pyrene fluorescence excimer to monomer ratio and the loss of ΔH at 60 mol % diheptanoyl-PC, it is evident that classical mixed micelles become the dominant structures at high mole fractions of diheptanoyl-PC. The point at which these mixed micelles form a single lipid phase has been determined by observing the ^{1}H NMR line width of dipalmitoyl-PC in mixtures (short-chain PC/long-chain PC $\geq$ 0.2) formed with diheptanoyl-PC-d_{26} (e.g., the species with both short chains perdeuterated). At temperatures below 38 °C, the line width of the bulk (CH_2) protons was moderately large ($\sim$150 Hz) in the small binary PC bilayer aggregates (Figure 7). As the proportion of short-chain PC was increased past 0.3–0.4 mol fraction (depending on the temperature), the line width decreased rapidly. This is consistent with either fast exchange of the dipalmitoyl-PC between the small bilayer particles and classical mixed micelles or a continuous change in the size and mobility of the gel-state dipalmitoyl-PC-containing particles.

At higher short-chain PC mole fractions, the line width decreased still further, but more slowly. This region is composed of classical diheptanoyl-PC/dipalmitoyl-PC mixed micelles which are decreasing slightly in size with increasing short-chain PC concentration. Both of these regions can be fit with straight lines and their intersection used to define the composition at which mixed micelles become the sole species. This value is relatively constant below 30 °C; at temperatures above 30 °C, the pure mixed micelle phase occurs at lower mole fraction diheptanoyl-PC. This information for several temperatures can be used to construct the boundary line for the mixed micelle phase.

Discussion

Phase Separation in PC Bilayers and Reversible Fusion. The spatial arrangement of the two components in diheptanoyl-PC/dipalmitoyl-PC particles is critical to understanding their stability and unusual phase behavior. While the temperature-induced fusion of the small particles above T_m (Eum et al., 1989) could be rationalized if the two species were phase-separated below the T_m of the long-chain component, no concrete evidence for this existed. We have used a number of techniques to support the phase separation model of the short-chain PC/gel-state dipalmitoyl-PC particles. Pyrene fluorescence data suggest that at low ratios of diheptanoyl-PC to dipalmitoyl-PC there is some degree of phase separation of both components. This is also consistent with the DSC results where even at higher mole fractions of diheptanoyl-PC a ΔH for the gel-to-liquid-crystalline transition is still observed. For 20–40 mol % diheptanoyl-PC, the relatively constant magnitude of ΔH is comparable to what is cited for small unilamellar vesicles of dipalmitoyl-PC. The ^2H NMR spectra for the chain-perdeuterated short-chain PC in excess gel-state dipalmitoyl-PC exhibited an isotropic peak at room temperature, but a distinct quadrupole splitting for CD_2 groups only after heating the sample above the dipalmitoyl-PC T_m. Even when the short-chain PC was 5% of the total lipid, it did not mix into the gel-state DPPC, again indicating phase separation. The net result is that the small particles which form in the range 20–40 mol % diheptanoyl-PC have dipalmitoyl-PC bilayer characteristics (ΔH and T_m); hence, they must have the bulk of the diheptanoyl-PC spatially distinct from the gel-state dipalmitoyl-PC. The stability of these small gel-state PC particles is compromised when the temperature is raised to the T_m of the long-chain component. At that point, it is expected that the short-chain PC will mix randomly with the liquid-crystalline long-chain PC. If the phase-separated short-chain PC is necessary to stabilize the small particles, which is expected since small bilayers of pure dipalmitoyl-PC below T_m are unstable, then when phase separation no longer occurs the small bilayers will fuse to large structures. Reversibility for such a system would be expected as soon as the temperature was lowered and the two components began to separate again.

Phase Diagram for Diheptanoyl-PC/Dipalmitoyl-PC Particles. The diheptanoyl-PC/dipalmitoyl-PC system exhibits a complex variety of structures (nearly pure dipalmitoyl-PC multibilayers, mixed lipid multibilayers, small bilayer aggregates, and classical mixed micelles) depending on the ratio of the two components and the system temperature. The information presented in this work can be used to construct a composition/temperature phase diagram (Figure 8). The maximum point in the plot of excimer/monomer intensity ratio with composition is taken as the point at which the multibilayer structures disappear and small bilayer aggregates become the only structure present. The end of the drop in the intensity

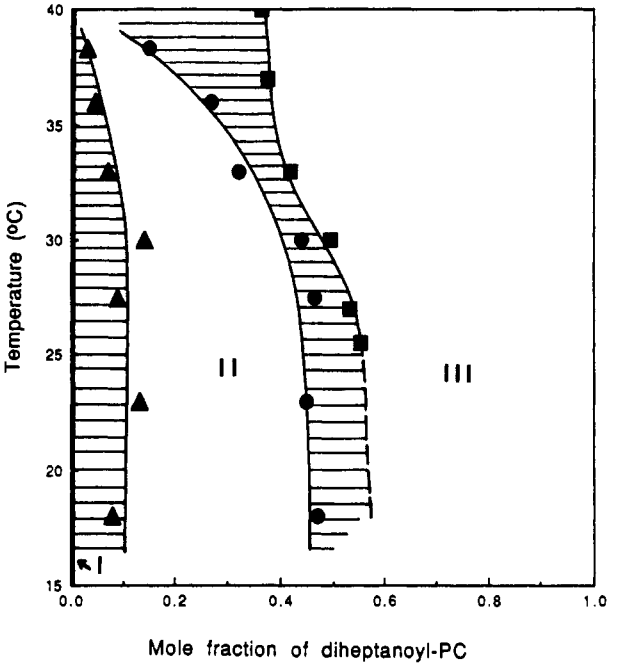

FIGURE 8: Temperature phase diagram for the two-component system of diheptanoyl-PC and dipalmitoyl-PC (25 mM total lipid). There are three discrete phases: region I, multibilayers of dipalmitoyl-PC with <0.01 mol fraction diheptanoyl-PC; region II, small bilayer particles (~90-Å R_H); and region III, classical mixed micelles. The boundary for the disappearance of the multibilayers coexisting with the pure small bilayer particle phase (▲) was determined from the maximum excimer fluorescence intensity ratio I_{466}/I_{392} as described in the text; the boundary indicating the coexistence of classical mixed micelles with small bilayer particles (●) was determined from the minimum I_{466}/I_{392} ratio; the boundary indicating a pure classical mixed micelle phase (■) was determined from the ^1H line-width data in Figure 7.

ratio signals the appearance of classical mixed micelles in which the dipalmitoyl-PC exhibits no ΔH. Definition of the points at which only classical mixed micelles exist is done from the dipalmitoyl-PC line width versus composition studies. The coexistence of bilayer particles and mixed micelles between 40 and 60 mol % short-chain PC is supported by light-scattering results (Eum et al., 1989) where the larger bilayer particles disappear somewhere between 50 and 67 mol % diheptanoyl-PC. The heat of the gel-to-liquid-crystalline phase transition of dipalmitoyl-PC cannot be detected by DSC when the short-chain PC is 60 mol %. This is also consistent with the disappearance of bilayer particles at that composition. A pronounced change in the phase lines (toward lower mole fraction diheptanoyl-PC) for small bilayer particles occurs above 30 °C. This temperature is near the pretransition of a pure dipalmitoyl-PC phase. The change in the headgroup orientation of the long-chain PC with temperature presumably increases the solubility of the long-chain species in diheptanoyl-PC domains. This is supported by the fact that the drop in excimer to monomer ratio in pure dipalmitoyl-PC does not occur at the main transition temperature but around 30 °C (Galla & Sackman, 1974). The effect of increasing the temperature above 30 °C has a much smaller effect on formation of classical mixed micelles. Above 38–40 °C, particles with 20–50 mol % diheptanoyl-PC fuse to large structures (Eum et al., 1989) with smaller amounts of dipalmitoyl-PC in small particles in the soluble phase (Bian et al., unpublished work). For mixtures with less than 33 mol % diheptanoyl-PC, there is no lysis of erythrocytes by these particles, indicating that classical-type mixed micelles are not present (Riedy et al., 1990). With this phase diagram in mind, we can reinterpret

the complex pyrene excimer/monomer versus composition curve for fixed pyrene/diheptanoyl-PC at 25 °C (Figure 5B). Referring to DSC and results from other techniques, four regions of different curvature can be discerned in that plot. These are interpreted in the following way. (i) At <20 mol % diheptanoyl-PC, multibilayers coexist with small bilayer aggregates. At very low amounts of diheptanoyl-PC, the pyrene is partitioned into the gel-state dipalmitoyl-PC region, and microcrystals of pyrene presumably exist. As the short-chain PC is added, the microcrystals are dissolved and the pyrene solubilized in the diheptanoyl-PC domains of the small bilayer particles. (ii) In the range 20–42 mol % diheptanoyl-PC, the short-chain PC domains in the small bilayer particles grow with additional diheptanoyl-PC. Since the pyrene is preferentially partitioned into this liquid-crystalline milieu, a small increase in excimer formation is observed. (iii) Between 42 and 56 mol % diheptanoyl-PC, the slope is almost linear since additional short-chain PC (with same ratio of pyrene) only increases the number of mixed micelles with the same size. (iv) After 56 mol % diheptanoyl-PC, only mixed micelles exist—the slope in this section is larger and probably reflects the decreased viscosity in smaller diheptanoyl-PC mixed micelles compared to the diheptanoyl-PC domains in small bilayer aggregates.

Geometrical Models of Bilayer Particles. The most interesting particle in the phase diagram for this binary PC mixture is the small bilayer aggregate where the diheptanoyl-PC is extensively phase-separated from gel-state dipalmitoyl-PC (20–42 mol % short-chain PC). These small (90-Å R_H) particles are known to be nonlytic to human erythrocytes (Gabriel et al., 1987); hence, they cannot be like classical rod-shaped short-chain PC micelles. For these particles, additional short-chain PC appears to increase the size of the diheptanoyl-PC domains. The modulus of bending elasticity for a bilayer membrane is on the order of tens of kT (Szleifer et al., 1988); for the gel-state dipalmitoyl-PC, the curvature energy would be very large for such small (90-Å, R_H) vesicles and possibly beyond the limit of elasticity (resulting in breakage of such highly curved structures). If the curvature radius of the vesicles were near the bilayer thickness (presumably ~45 Å for a gel-state dipalmitoyl-PC bilayer), it would be almost impossible for gel-state dipalmitoyl-PC to form and remain stable in such a small sphere. Thus, any vesicles that exist at such small sizes must be flattened and closer to oblate particles with the diheptanoyl-PC located in the equatorial area between the two dipalmitoyl-PC bilayer segments. In such a model, the short-chain PC acts like glue to bind the two gel-state dipalmitoyl-PC bilayers together. (Another type of bilayer structure, where unilamellar vesicles are formed with long-chain PC molecules interdigitated and the diheptanoyl-PC localized in clusters on the outer layer, could also be constructed, although there is no precedence for this sort of interdigitation.) It is probable that some dipalmitoyl-PC is "dissolved" in the fluid diheptanoyl-PC. Some of the bilayer aggregates may also exist as single disks with the short-chain PC stabilizing the edge of dipalmitoyl-PC bilayer pieces. Such particles would be similar in geometry to the bile salt/lecithin disks formed at high ratios of bile salt to PC (Schurtenberger et al., 1985; Schubert & Schmidt, 1988). The disks in that system occur when the bile salt is 0.6–0.8 mol fraction total lipid, whereas with diheptanoyl-PC the ratio is 0.2–0.4. The driving force for formation of single disks rather than enclosed structures is mainly entropic. The micellelike diheptanoyl-PC prevents the hydrocarbon of the edges of bilayers from contacting water, and the large bilayer

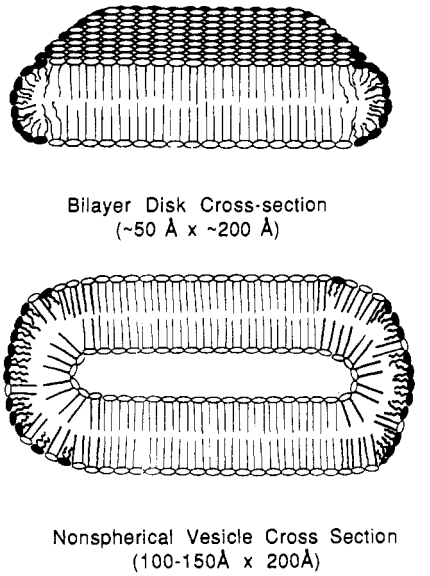

FIGURE 9: Models for the small bilayer particles detected in the range 0.2–0.4 mol fraction diheptanoyl-PC: bilayer disk and nonspherical vesicle. Both structures have been cut in half to illustrate the arrangement of the two PC species. In the nonspherical vesicle, the bulk of the short-chain PC is on the exterior surface, consistent with experimental evidence. The dark headgroups indicate short-chain PC molecules.

forms particles as small as possible to increase the system entropy if there is sufficient diheptanoyl-PC to eliminate the edge effect of small bilayers.

The different types of small bilayer structures are shown in Figure 9. If two small bilayers from a vesicle, it will reduce the amount of diheptanoyl-PC needed to stabilize the particle but cost curvature energy. Both effects should depend on the relative ratio of dipalmitoyl-PC to diheptanoyl-PC, but not on the total amount of lipids. Previous studies have indicated that the bulk of the short-chain PC is accessible to the exterior solution (Gabriel & Roberts, 1986); therefore, in the arrangement of the nonspherical vesicle, most of the diheptanoyl-PC must be on the exterior surface. The existence of these particles can explain the low entrapment volumes of 4:1 dipalmitoyl-PC/diheptanoyl-PC mixtures in the following manner. Either (i) small, nonspherical, compressed vesicles are the major components with few if any disks (these clearly have reduced internal volumes compared to spherical vesicles), (ii) small vesicles (presumably nonspherical) which entrap material and disks coexist, or (iii) the population is mostly disks with a small population of large vesicles with larger encapsulation volumes. There were no large vesicle structures in negative-stained EM micrographs of diheptanoyl-PC/dipalmitoyl-PC particles (Gabriel & Roberts, 1986); hence, either of the first two explanations may be more probable. The disk structures would be unique as nonvesicular particles which do not cause lysis of red blood cells, even though they have a region of micellelike phase-separated short-chain PC. The conversion from nonspherical vesicles or nonlytic disks to mixed micelles occurs at a certain critical ratio of diheptanoyl-PC. At this point, most of the long-chain PC would be solubilized in the exterior short-chain PC with insufficient molecules for a gel-state bilayer domain in the disk. The disks would collapse to classical micelles whose interaction with erythrocytes releases hemoglobin.

Phospholipase Action toward Binary PC Particles. The binary PC particles have unique kinetic features when used as substrates for both phospholipase A_2 and C: (i) preferential hydrolysis of the short-chain PC below T_m with kinetic pa-

rameters similar to those for pure micelle; (ii) only a fraction of the total short-chain PC is hydrolyzed by both enzymes in particles incubated above T_m; and (iii) the available short-chain PC is not much better as a substrate for phospholipase A_2 than the long-chain PC matrix in particles incubated above T_m. Each of these observations can be understood with a detailed model for the particles and a knowledge of the composition phase behavior. The high V_{max} for both enzymes (a factor of 2 less than the V_{max} for pure micelles) toward diheptanoyl-PC below T_m is toward diheptanoyl-PC in domains which are separated from the gel-state long-chain PC bilayer matrix. The short-chain PC is in a micellelike environment even in these bilayer particles. Since both enzymes increase in specific activity above 40 mol % short-chain PC, where classical mixed micelles coexist with the small bilayer particles, the environment of the diheptanoyl-PC in the small bilayers is not quite as free as in the pure rod-shaped short-chain PC micelles.

The decrease in the total amount of diheptanoyl-PC hydrolyzed by PLC in 20 mol % particles above T_m (from 95% to 21% at 45 °C) can be quantitatively understood in terms of the partitioning of the short-chain PC between multilamellar particles and smaller structures which appear isotropic in the ^2H NMR experiment. Only substrate in the smaller particles is available to the enzymes, thus reducing the total amount of diheptanoyl-PC hydrolyzed. These new structures have liquid-crystalline dipalmitoyl-PC mixed (presumably randomly) with the diheptanoyl-PC. Phospholipase A_2 rates decrease toward the diheptanoyl-PC in these particles—activity is also low toward egg PC/diheptanoyl-PC particles; phospholipase C rates are not affected in these same situations whereas the extent of PC hydrolysis is. This strongly suggests for the former enzyme, intermolecular PC/PC interactions are kinetically more important than for phospholipase C.

ACKNOWLEDGMENTS

The ^2H NMR spectra were acquired at the California Institute of Technology with the help of Dr. Gerard Riedy and Dr. Paula Watnick.

Registry No. Dipalmitoylphosphatidylcholine, 63-89-8; diheptanoylphosphatidylcholine, 39036-04-9.

REFERENCES

Birks, B. (1970) *Photophysics of Aromatic Molecules*, Wiley-Interscience, London.

Birks, J. B., Dyson, D. J., & Munro, I. H. (1963) *Proc. R. Soc. London A275*, 575–585.

Brown, M. F., & Davis, J. H. (1981) *Chem. Phys. Lett. 79*, 431–435.

Burns, R. A., Jr., Donovan, J. M., & Roberts, M. F. (1983) *Biochemistry 22*, 964–973.

Chong, P. L., & Thompson, T. E. (1985) *Biophys. J. 47*, 613–621.

DeBose, C. D., Burns, R. A., Jr., Donovan, J. M., & Roberts, M. F. (1985) *Biochemistry 24*, 1298–1306.

Eum, K. M., Riedy, G., Langley, K. H., & Roberts, M. F. (1989) *Biochemistry 28*, 8206–8213.

Forster, Th. (1969) *Angew. Chem. 8*, 333–343.

Gabriel, N. E., & Roberts, M. F. (1984) *Biochemistry 23*, 4011–4015.

Gabriel, N. E., & Roberts, M. F. (1986) *Biochemistry 25*, 2812–2821.

Gabriel, N. E., & Roberts, M. F. (1987) *Biochemistry 26*, 2432–2440.

Gabriel, N. E., Agman, N. V., & Roberts, M. F. (1987) *Biochemistry 26*, 7409–7418.

Galla, H.-J., Sackman, E. (1974) *Biochim. Biophys. Acta 339*, 103–115.

Hauser, H., Gains, N., & Mueller, M. (1983) *Biochemistry 22*, 4775–4781.

Kim, J.-S., Kim, C.-K., Song, P.-S., & Lee, K.-M. (1981) *J. Colloid Interface Sci. 80*, 284–287.

Lichtenberg, D., Freire, E., Schmidt, C. F., Barenholz, Y., Felgner, P. L., & Thompson, T. E. (1981) *Biochemistry 20*, 3462–3467.

Lin, T.-L., Chen, S.-H., Gabriel, N. E., & Roberts, M. F. (1987) *J. Phys. Chem. 91*, 406–413.

Moigne, J. L., Sturm, J., & Zana, R. (1988) *J. Phys. Chem. 89*, 2709–2713.

Roberts, M. F., & Gabriel, N. E. (1988) *Colloid Surf. 30*, 113–132.

Schubert, R., & Schmidt, K.-H. (1988) *Biochemistry 27*, 8787–8794.

Schullery, S. E., Schmidt, C. F., Felgner, P., Tillack, T. W., & Thompson, T. E. (1980) *Biochemistry 19*, 3919–3923.

Schurtenberger, P., Mazer, N., & Kanzig, W. (1985) *J. Phys. Chem. 89*, 1042–1049.

Szleifer, I., Kramer, D., Ben-Shaul, A., Roux, D., & Gelbart, W. M. (1988) *Phys. Rev. Lett. 60*, 1966–1969.

Tausk, R. J. M., Karmiggelt, J., Oudshoorn, C., & Overbeek, J. Th. G. (1974) *Biophys. Chem. 1*, 175–183.

Vold, R. L., Waugh, J. S., & Klein, M. P. (1968) *J. Chem. Phys. 48*, 3831–3839.

Watnick, P. I., Dea, P., & Chan, S. I. (1990) *Proc. Natl. Acad. Sci. U.S.A. 87*, 2082–2086.